Collective Resonance Model of Energy Exchange in 3D Nonequipartitioned Beams

I. Hofmann
GSI Darmstadt, Planckstrasse 1, 64291 Darmstadt, Germany

J. Qiang and R. D. Ryne
Los Alamos National Laboratory, Los Alamos, New Mexico 87545
(Received 28 June 2000)

Energy exchange between the longitudinal and transverse degrees of freedom of nonequipartitioned bunched beams (non-neutral plasmas) is investigated by means of 3D simulation. It is found that collective instability may lead to energy transfer in the direction of equipartition, without full progression to it, in certain bounded regions of parameter space where internal resonance conditions are satisfied, in good agreement with stability charts from an earlier derived 2D Vlasov analysis. Nonequipartitioned stable equilibria, however, exist in relatively wide regimes of parameter space. This provides evidence that such regimes may be safely used in the design of future high-intensity linacs.

DOI: 10.1103/PhysRevLett.86.2313 PACS numbers: 29.27.Bd, 29.17.+w, 41.75.–i

Energy exchange in an anisotropic ensemble of charged particles confined by a harmonic potential and interacting via the self-consistent space charge potential is of basic interest in non-neutral plasmas. The use of nonequipartitioned bunched beams is also an important issue in the design of future high-intensity linear accelerators, about which different authors have come to partly contradictory conclusions. Linac design studies by Jameson [1,2] have suggested that nonequipartitioned beams are not subject to emittance dilution in certain regions of parameter space, while in other regions equipartitioned beams appeared to be advantageous. The "thermodynamic model" proposed by Reiser [3,4] assumes that beams always relax to energy equipartition. Along this line Kishek *et al.* [5] have recently found simulation results for anisotropic 2D beams in symmetric focusing systems which they interpret as support of the thermodynamic model.

Thermal equilibrium states have been applied to collisional plasmas including one-component plasmas in traps [6]. For linear accelerators, however, collisions are practically absent, with some limitations as recently shown by Gluckstern and Fedotov [7]; hence the self-consistent electric field remains to provide coupling. Although thermodynamic considerations can be useful to describe emittance growth in special systems as shown by O'Shea [8], caution is required in general. This is due to the fact that statistical mechanics and thermodynamics of large Coulomb systems are based on Debye screening of the cumbersome long-range Coulomb potential at reasonably short distance [9], which is not fulfilled in our case except close to the space charge limit. The equipartition issue has also been discussed in the language of nonlinear dynamics of coupled oscillators to account for possible resonances in the external potential, with some analogy to the classical Fermi-Pasta-Ulam [10] problem of a chain of particles. Attempts to show the existence of a "strong stochastic threshold" have so far not been successful [11]. The fundamental difficulty with our problem is that the interaction part of the Hamiltonian cannot be written down explicitly due to the time-evolving nature of the self-consistent coupling force.

A comprehensive solution not restricted to specific parameters was proposed by Hofmann [12] in terms of a self-consistent "collective instability" analysis of the transverse 2D anisotropic Kapchinskij-Vladimirskij (KV) distribution in constant focusing systems with arbitrary asymmetry. Details of this perturbation theory were elaborated in Ref. [13], where it was shown that eigenmodes with nonlinear space charge coupling forces may grow exponentially in the vicinity of certain internal resonance conditions. Note that the unperturbed KV system has no coupling, and energy transfer cannot occur unless—as in real (or simulation) systems—some small initial density fluctuations lead to a finite nonlinear coupling force by an exponentially growing eigenmode. Eigenmodes are characterized by the order of the polynomial in x and y, which describes the perturbed space charge potential. In addition "free energy" is required for driving the instabilities, which stems from the energy anisotropy between different degrees of freedom. Such a "kinetic" effect leads to a substantial increase in the number of eigenmodes for a given order compared with isotropic or—even more—with fluid models. This explains why the modes considered here could not be found in beam transport studies using isotropic energy distributions or in fluid models of isotropic beams as in the applications given in Ref. [14]. Some of these collective anisotropy instabilities were confirmed by 2D simulations of KV and waterbag beams in Refs. [15] and [5]; the latter also describes the possibility of energy transfer in terms of density wave interaction in semi-Gaussian beams close to the space charge limit. Collective instability of longitudinally propagating waves in anisotropic coasting beams is also found in simulations by Haber *et al.* [16], although the absence of a longitudinal confining potential makes a significant difference. The results of the 2D analytical work are conveniently expressed in 2D "stability charts" (see also Ref. [2]) in terms of three independent parameters, the emittance ratio for a given chart, the "tune" ratio expressing the resonance features, and the tune depression in one direction as a measure for space charge. Here the tune ν_0 (in x, y, z) is the oscillation frequency in the absence of space charge, and ν is the corresponding space charge depressed value. Note that the energy anisotropy between planes x and y is defined as a ratio of kinetic energies, which can be expressed as $T \equiv (\epsilon_x \nu_x)/(\epsilon_y \nu_y)$ for harmonic oscillators.

Following Ref. [13] (with x and y interchanged), a case for an emittance ratio of 2—typical for linac design—is calculated in Fig. 1, which will subsequently be used to interpret our simulations by relating y to the longitudinal z. Parameter regions predicting instability of eigenmodes are marked for third and fourth order modes. Note the pronounced resonance structure for not too strong tune depression ($\nu_x/\nu_{0x} \gtrsim 0.4$). For $\nu_x/\nu_{0x} \rightarrow 1$ we find for the stronger nonoscillatory modes $\nu_y - 2\nu_x \approx 0$ in third order, and in fourth order $\nu_y - 3\nu_x \approx 0$, $2\nu_y - 2\nu_x \approx 0$, as well as the very narrow $\nu_x - 3\nu_y \approx 0$. The proper resonance conditions include a coherent tune shift, which causes broadening of the resonance bands with increasing intensity. For stronger tune depression we notice "resonance overlap": instability is present for all tune ratios in a "sea of instability" which may be related to a strong stochastic threshold. Note that this limit of vanishing resonance structure also coincides with the limit where the Debye screening length—given roughly by $\lambda_D/a \lesssim \nu/\nu_0$ [17]—is small compared with the bunch dimension a.

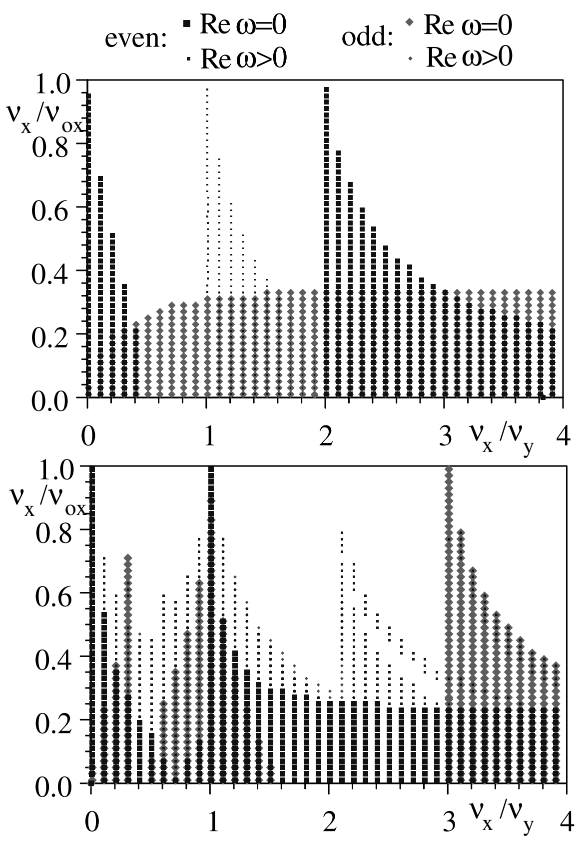

FIG. 1. 2D stability charts for fixed $\epsilon_y/\epsilon_x = 2$ as a function of betatron tune ratio and tune depression ($\nu_y/\nu_x = 1/2$ pertains to equipartition). Markers indicate the presence of instabilities of third order (top graph) and fourth order (bottom graph), with a distinction between even and odd mode symmetry as well as nonoscillatory (Re$\omega = 0$) and oscillatory eigenfrequencies (Re$\omega > 0$), where the latter generally have noticeably smaller growth rates.

To carry out the 3D-2D comparison (relating the z direction in 3D to y in 2D) we use the fully 3D particle-in-cell (PIC) code IMPACT [18]. The simulations were performed on parallel processors using two million macroparticles; the space charge calculation was performed using a $64 \times 64 \times 64$ spatial grid to contain the beam bunch. Computationally, a doubled grid was used, with a modified Green function, to solve the Poisson equation with open boundary conditions. For our purpose the choice of nonequipartitioned initial distributions in 3D requires some thought. For equipartitioned beams Gluckstern [19] describes a class of exact equilibria as functions of the Hamiltonian. Such an approach, however, does not provide the freedom to generate nonequipartitioned beams. We therefore introduce anisotropy by adjusting and matching rms moments, which leaves an inevitable initial density mismatch containing fourth, sixth, and higher order modes. Note that all quantities like tunes or emittances are defined as rms values. The issue of energy exchange driven by rms mismatch is a separate one, with some aspects recently discussed in Ref. [20]. For weak or moderate space charge (as in most linacs) the rms-matched waterbag distribution appears to be more suitable than a semi-Gaussian distribution (uniform real density) which is strongly mismatched at the beam boundary; close to the space charge limit ($\nu/\nu_0 \ll 1$), however, a uniform density is the natural limit.

The resonance feature of the instabilities in 3D simulations is most clearly verified for parameters where third order modes are expected. These are not excited by our choice of initial distribution—except on a noise level—hence exponential growth should be visible. If we take a focusing system with $\nu_{0z}/\nu_{0x} = 1.5$ and increase the current beyond the threshold where the resulting parameter trajectory in Fig. 1 crosses the stop-band edge at $\nu_z/\nu_x = 2$ we expect the onset of instability. The energy anisotropy $T \equiv (\epsilon_z \nu_z)/(\epsilon_x \nu_x)$ is 4 at this particular point. The simulation shows that for $\nu_z/\nu_x = 1.96$ there is negligible emittance change (<3% which stems from initial mismatch) over 200 transverse periods. Slightly above the threshold ($\nu_z/\nu_x = 2.04$) we find a phase of modest energy exchange after about period 50 which saturates at about period 200 and reduces the anisotropy from $T = 4.1 \rightarrow 2.6$ (top of Fig. 2). The self-limiting energy exchange far from equipartition can be explained by detuning after the working point drops below $\nu_z/\nu_x = 2$ due to emittance exchange—a typical resonance phenomenon. For higher currents the exponential growth is accentuated; it occurs in only a few

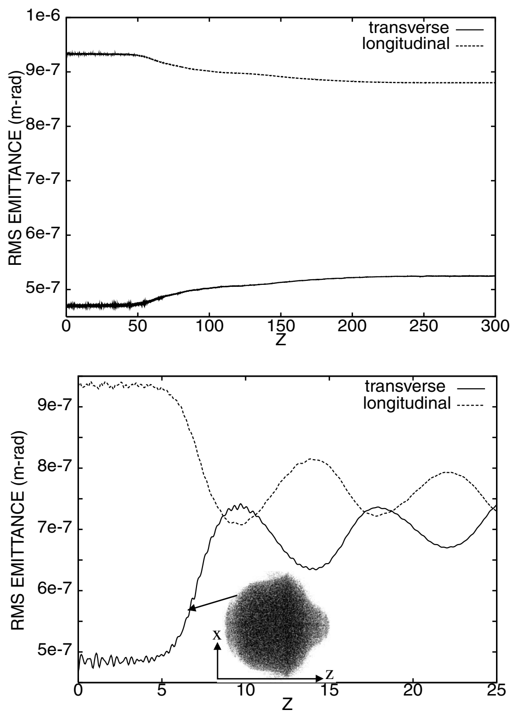

FIG. 2. rms emittances (upper trace in z, lower in x) for $\epsilon_z/\epsilon_x = 2$ (waterbag), $\nu_{0z}/\nu_{0x} = 1.5$, inside the resonance band of third order. Top: $\nu_z/\nu_x = 2.04$ ($T = 4.1 \rightarrow 2.6$); bottom: $\nu_z/\nu_x = 2.94$ ($T = 5.9 \rightarrow 1.6$). Units in z are transverse single particle periods without space charge ($z - x$ scatter plot at period 6).

periods for $\nu_z/\nu_x = 2.94$, where the energy anisotropy drops from 5.9 to about 1.6, hence again without reaching equipartition (bottom of Fig. 2). In the emittance evolution an x-y exchange occurs between period 50 and 100, and final saturation is reached near period 100. Comparison with results from a semi-Gaussian initial distribution have shown the same threshold behavior and exponential growth at a comparable rate. Note that Fig. 2 (bottom) shows a small ($\approx$5%) growth of the transverse emittance during a fraction of the first period of oscillation, which is similar for the initial semi-Gaussian. We relate this growth to the nonlinear field energy from initial density redistribution [17].

The real space projection into z-x in the exponential phase shows the typical "triangular" symmetry, which can be related to the third order (even) mode of the 2D theory [13]. A similar feature is found for the focusing system $\nu_{0z}/\nu_{0x} = 1.2$ for currents exceeding $\nu_z/\nu_x = 2$, but less pronounced for $\nu_{0z}/\nu_{0x} = 1.7, \ldots, 1.9$, where the crossing of the resonance takes place at a lower space charge level.

A 3D stability chart mapping the same plane as in Fig. 1 is shown in Fig. 3 by considering different focusing systems defined by ν_{0z}/ν_{0x}, and expressing beam current in terms of ν_x/ν_{0x}. Most cases have been run to a distance corresponding to 50–100 transverse periods, which was generally enough to reach saturation of the observed phenomena. The markers are related to emittance growth in the originally "colder" direction (in z for $T < 1$ and

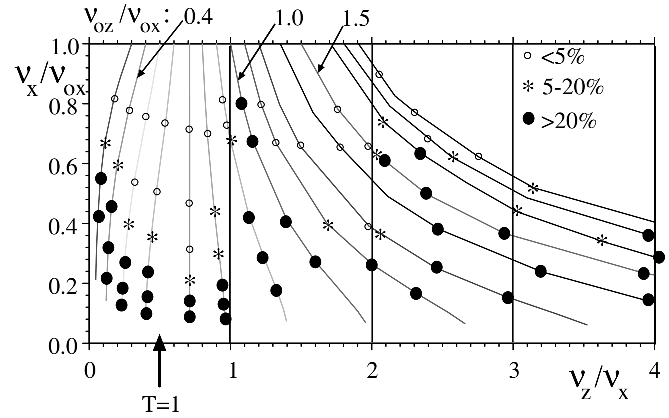

FIG. 3. Simulation results for initial $\epsilon_z/\epsilon_x = 2$ (waterbag); markers indicate level of emittance growth in the initially colder direction (lines connecting markers indicate same focusing system ν_{0z}/ν_{0x} defined by the zero current value at $\nu_x/\nu_{0x} = 1$).

in x, y for $T > 1$). We introduce three levels: "<5%" stands for "stable," the transition region with "5%–20%" for low-level growth, and ">20%" for pronounced growth. There is good agreement with the topology of Fig. 1: emittances remain practically constant (within 0%–5%), irrespective of T, except in the resonant bands attached to $\nu_z/\nu_x = 1, 2$; for $\nu_z/\nu_x \ll 1$ and sufficiently high current (such that $\nu_z/\nu_{0z} \ll 1$) as well as unconstrained in ν_z/ν_x for strong tune depression in x. This finding is essential for our study, as it confirms in retrospect the existence of anisotropic quasistationary equilibria in 3D and allows the discussion of stability properties for waterbag and semi-Gaussian distributions.

A third order resonance might also be expected for $2\nu_z/\nu_x = 1$, yet this case is equipartitioned in agreement with Fig. 1; likewise no effect is seen in the simulations. Furthermore, we see no exchange at the predicted very narrow fourth order resonance at $3\nu_z/\nu_x = 1$, which may be explained by easy detuning. We mention that this resonance topology for an initial emittance ratio of 2 is subject to changes for other emittance ratios [13].

The results for the symmetric focusing system $\nu_{0z}/\nu_{0x} = 1$ require additional comment and need to be compared with the 2D symmetric focusing study of Ref. [5]. Contrary to the system $\nu_{0z}/\nu_{0x} = 1.5$, which crosses through a resonance band at a certain current, we now find energy transfer at all current levels. In Fig. 4 the exchange takes off immediately, indicating that the instability starts already beyond its early exponential phase, and with several modes, as may be expected from the presence of even order modes in the initial density profile mismatch. Note that typical e-folding times for single modes according to Ref. [13] are three periods. The final emittance as well as energy ratio saturate at 1.3 for all simulated currents of the waterbag; in a semi-Gaussian cross-check with $\nu_x/\nu_{0x} = 0.41$ the saturation is at about 1.2. Our simulation findings thus reflect quite similar features as the 2D semi-Gaussian studies of Ref. [5] although we do not observe full equipartitioning. The

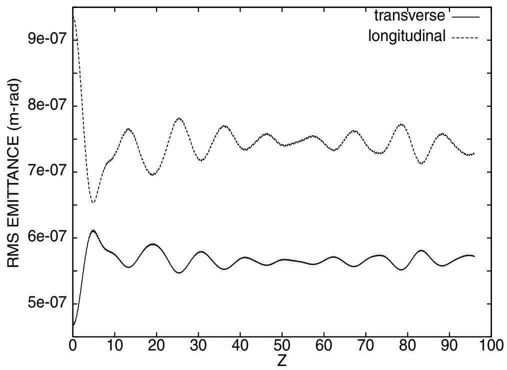

FIG. 4. Symmetric focusing $\nu_{0z}/\nu_{0x} = 1$, $\nu_z/\nu_x = 1.16$ ($\nu_x/\nu_{0x} = 0.68$) (waterbag; with T:2.3 → 1.3).

observation, however, in Ref. [5] that the KV case for weak space charge ($\xi = 0.87$) should be stable by theory as well as simulation—which would place it in contrast to the semi-Gaussian—is not confirmed by us. Correct evaluation of the 2D dispersion relations of Ref. [13] yields an e-folding in eight periods; we have conducted a 2D simulation sufficiently long to contain several e-foldings and found the predicted instability with equipartitioning. We thus reemphasize the conclusion that the behavior of nonequipartitioned KV beams is confirmed by the more realistic beams studied in the present paper.

The initially equipartitioned case $\nu_z/\nu_x \approx 0.5$ shows no emittance or energy exchange, but growth occurs equally in z and x for strong tune depression. For orientation we mention that for rms matched spherical waterbag beams rapid emittance growth—within less than a betatron period—due to conversion of nonlinear field energy from density mismatch is readily calculated as 20% for a tune depression of $\nu/\nu_0 = 0.2$ and continues to grow with increasing space charge [17]. A similar theoretical model applied to ellipsoidal or anisotropic bunches is not available. Hence, it is difficult to quantitatively distinguish emittance growth caused by density mismatch from the effect of instability in the limit of small ν_x/ν_{0x} or ν_z/ν_{0z}. The latter is the longitudinal space charge limit which occurs for weak longitudinal focusing strength; note that for $\nu_z/\nu_x < 0.5$ the energy anisotropy is reversed, and Fig. 1 predicts instability for small ν_z/ν_x and moderate ν_x/ν_{0x}. The simulation emittance growth in this limit cannot easily be related to a resonance of particular order, since according to Fig. 1 bands for third order modes at $\nu_y \approx 0$ and fourth order modes at $3\nu_y - \nu_x \approx 0$ practically overlap, and the effect of resonance is mixed with the nonlinear field energy issue. We have studied this in some detail for the focusing system $\nu_{0z}/\nu_{0x} = 0.4$. For the case $\nu_x/\nu_{0x} = 0.45$, $\nu_z/\nu_{0z} = 0.1$ (>20% in Fig. 3) a slow approach to equipartition follows an initial growth with rapid oscillations from density mismatch. A cross-check of this case using the SCOPXYZ PIC code and suppressing the initial density mismatch effect by adiabatically raising the intensity has shown the same transition from <20% to >20% in the longitudinal emittance growth [21].

We summarize our results in essentially two categories: (1) For moderate space charge, energy transfer towards equipartition is found in low (third and fourth) order collective resonances well described by the 2D KV theory.

(2) For strong tune depression the resonance structure vanishes: energy exchange approaching or reaching equipartition is not restricted to certain tune ratios. This "plasma" region in the proper sense of the word ($\lambda_D \ll a$) merits further study to explore the role of plasma oscillations or density waves.

The implication of Ref. [5] that equipartition may be a universal feature is thus not supported by our work. With respect to high-current linac design we find extended "safe" areas in parameter space, but resonance bands near integer tune ratios—in particular, crossing of $\nu_z/\nu_x = 1$—and strong tune depression ($\nu_x/\nu_{0x} \lesssim 0.4$) should be avoided. The additional design freedom may be used to minimize cost.

The authors acknowledge critical comments on the manuscript by R. A. Jameson and discussions with M. Reiser. This work was performed using resources of the NERSC and ACL scientific computing centers located at LBNL and LANL, respectively.

[1] R. A. Jameson, IEEE Trans. Nucl. Sci. **28**, 2408 (1981).
[2] R. A. Jameson, in *Advanced Accelerator Concepts,* edited by J. S. Wurtele, AIP Conf. Proc. No. 279 (AIP, New York, 1993), p. 969.
[3] M. Reiser and N. Brown, Phys. Rev. Lett. **74**, 1111 (1995).
[4] M. Reiser, *Theory and Design of Charged Particle Beams* (Wiley-Interscience, New York, 1994).
[5] R. A. Kishek, P. G. O'Shea, and M. Reiser, Phys. Rev. Lett. **85**, 4514 (2000).
[6] T. M. O'Neil and D. H. E. Dubin, Phys. Plasmas **5**, 2163 (1998).
[7] R. L. Gluckstern and A. V. Fedotov, Phys. Rev. ST Accel. Beams **2**, 054201 (1999).
[8] P. G. O'Shea, Phys. Rev. E **57**, 1081 (1998).
[9] E. H. Lieb, Rev. Mod. Phys. **48**, 553 (1976).
[10] J. Ford, Phys. Rep. **213**, 271 (1992).
[11] J-M. Lagniel and S. Nath, in *Proceedings of the European Particle Accelerator Conference, Stockholm, 1998* (Institute of Physics Publishing, Bristol, UK, 1998), p. 1118.
[12] I. Hofmann, IEEE Trans. Nucl. Sci. **28**, 2399 (1981).
[13] I. Hofmann, Phys. Rev. E **57**, 4713 (1998).
[14] S. M. Lund and R. C. Davidson, Phys. Plasmas **5**, 3028 (1998).
[15] I. Hofmann, Nucl. Instrum. Methods **187**, 281 (1981).
[16] I. Haber *et al.,* Fusion Eng. Des. **32–33**, 169 (1996).
[17] I. Hofmann and J. Struckmeier, Part. Accel. **21**, 69 (1987).
[18] J. Qiang *et al.,* J. Comput. Phys. **163**, 434 (2000).
[19] R. L. Gluckstern *et al.,* Phys. Rev. E **58**, 4977 (1998).
[20] I. Hofmann, Ji Qiang, and R. Ryne, in *Proceedings of the 1999 Particle Accelerator Conference, New York City* (IEEE, Piscataway, NJ, 1999), p. 137.
[21] R. W. Hasse (private communication).